INTERNATIONAL JOURNAL OF REFRIGERATION 40 (2014) 370–379

Available online at www.sciencedirect.com

ScienceDirect

journal homepage: www.elsevier.com/locate/ijrefrig

Modulation characteristics of a linear compressor for evaporating and condensing temperature variations for household refrigerators

Jong Kwon Kim [a], *Jong-Bong Kim* [b,*]

[a] *Product Testing Lab, LG Electronics, Digital Park, Pyeongtaek City, Gyeonggi 19-1, Republic of Korea*
[b] *Dept. of Mech. & Automotive Eng., Seoul National University of Science & Tech., Gongneung-Dong, Nowon-Gu, Seoul 139-743, Republic of Korea*

ARTICLE INFO

Article history:
Received 19 March 2013
Received in revised form
8 December 2013
Accepted 10 December 2013
Available online 19 December 2013

Keywords:
Linear compressor
Free piston
Household refrigerator
Refrigerating system
Modeling

ABSTRACT

Linear compressors are sensitive to both condensing and evaporating temperatures since they do not have mechanical restrictions to piston movement. Linear compressors used in refrigerators are subjected to a wide range of compression loads, because of the condensing temperature change caused by the ambient temperature variations and the evaporating temperature change due to the freezer compartment temperature. The compartment temperature is influenced by door opening, product loading, defrosting and setting temperature. This paper presents modulation characteristics of an inherent capacity-modulated linear compressor for evaporating temperature variations representing compartment temperature change. A numerical model and a prototype compressor were developed. The prototype compressor was evaluated over an evaporating temperature from −35 to −15 °C. The results were compared with the compressor performance variations over a condensing temperature from 30 to 50 °C. The cooling capacity increased by 241 and 50 W for 20 °C increment of the evaporating and condensing temperature, respectively.

Caractéristiques de modulation d'un compresseur linéaire pour des variations de température d'évaporation et de condensation de réfrigérateurs domestiques

Mots clés : Compresseur linéaire ; Piston libre ; Réfrigérateur domestique ; modélisation ; Systéme frigorifique

* *Corresponding author*. Tel.: +82 2 970 6434; fax: +82 2 979 7032.
E-mail address: jbkim@seoultech.ac.kr (J.-B. Kim).

0140-7007/$ – see front matter
http://dx.doi.org/10.1016/j.ijrefrig.2013.12.006

Nomenclature

A_p	cross sectional area of piston (m^2)
BDC	bottom dead center
C_f	friction damping coefficient (N ms^{-1})
c_t	total damping coefficient (N ms^{-1})
C	capacitance (μF)
CCR	cooling capacity ratio
COP	coefficient of performance
f_n	natural frequency (s^{-1})
f_{sys}	system resonant frequency (s^{-1})
F_{gas}	gas force (N)
i	current (A)
I_m	imaginary part
I	peak current (A)
k_{gas}	spring constant of gas (N m^{-1})
k_s	spring constant (N m^{-1})
k_t	total spring constant (N m^{-1})
L	inductance (mH)
m_p	mass of piston (kg)
P_c	pressure of cylinder chamber (Pa)
P_{dis}	pressure of discharge (Pa)
P_{suc}	pressure of suction (Pa)
$\dot{Q}$	cooling capacity (W)
Real	real part
R	resistance (Ω)
T	temperature (°C)
TDC	top dead center
υ	input voltage (V)
V	peak voltage (V)
$\dot{W}$	input power (W)
x	displacement (m)
X	peak displacement (m) reactance (Ω)
X_o	initial displacement (m)
$\dot{x}$	velocity (m s^{-1})
$\dot{x}_0$	initial velocity (m s^{-1})
$\ddot{x}_0$	acceleration (m s^{-2})
Z	impedance (Ω)

Greek letter

α	motor constant (N A^{-1})
θ	phase (degree)
θ_0	initial phase (degree)
ω	angular velocity (rad s^{-1})
ρ	refrigerant density (kg m^{-3})
η	efficiency

1. Introduction

A linear compressor has high efficiency characterized by its simple flow path, low friction loss, and highly efficient linear motor. On the other hand, compressor performance is sensitive to both condensing and evaporating temperature variations because the stroke of the piston, which does not have mechanical restrictions, is variable. Moreover, linear compressors used in home refrigerators are subjected to a wide range of compression loads associated with the evaporating and condensing temperature. The evaporating temperature is varied by door opening, product loading, defrosting, and freezer compartment temperature. The condensing temperature is influenced by the ambient temperature.

Lee et al. (2000) introduced a linear compressor for use in household refrigerators. They applied TRIACs, which controls the AC voltage in order to control the piston displacement of the compressor.

Lee et al. (2008) investigated a capacity modulated linear compressor under a wide range (50–100%) of cooling capacity. Since the stroke of a piston in the linear compressor is not fixed due to a mass-spring system, they defined the understroke as the difference between maximum piston stroke and reduced piston stroke for capacity modulation is called under-stroke. The cooling capacity was proportionally modulated by the under-stroke operation of the piston with a pulse width modulation (PWM) inverter. The linear compressor was operated with dead volume when the piston was in the under-stoke operation. It was shown that the varied dead volume was neither experimentally nor theoretically a dominant factor in determining the compression efficiency, because both the produced cooling capacity and the electrical energy input decrease at the same ratio. A comprehensive model of a linear compressor for electronics cooling was previously presented by Bradshaw et al. (2011) then proved the energy recovery characteristics of a linear compressor as compared to those of a reciprocating compressor. Bradshaw et al. (2013) showed that the overall isentropic efficiency of the linear compressor remained relatively unaffected by an increase in dead volume up to a certain point. It was analyzed that the linear compressor has a higher ability to store energy due to the higher stiffness of mechanical springs which is analogous capacitance in an electrical system. This characteristic behavior allows a linear compressor to be used for efficient capacity control roughly from 35 to 100%.

The present authors (Kim et al., 2009) previously investigated the dynamic characteristics in the range of the full capacity of a linear compressor. As the difference between the operating frequency and the natural frequency becomes greater, the COP of the linear compressor in the refrigeration cycle becomes accordingly lower. This means it is very important to link the operating frequency with the natural frequency for improvement of compressor efficiency. For the experiment in the aforementioned study, a PWM inverter was used to obtain the resonance system. The system consisted of a micro processor and electrical circuits. Power electronic elements were used to convert the AC power source to DC to induce a certain amount of AC power to reach to the motor. Piston controllers such as inverters and TRIACs are expensive to apply, need power to run, and require complicated control logic, since the piston movement is influenced by many different cycle conditions. Furthermore, for optimal performance and to minimize power consumption by

modulating the cooling capacity in accordance with the variable refrigerator conditions, a linear compressor driven by a position (piston) controller should be tuned specifically to the refrigeration cycle at each moment.

The present authors (Kim et al., 2011) also presented a novel design method for an inherent capacity modulated (ICM) linear compressor that uses R600a for application in household refrigerators. The prototype compressor was numerically evaluated over a condensing temperature range of 15–50 °C, which corresponds to an ambient temperature range of 5–43 °C. The design was validated experimentally at a condensing temperature range of 35–50 °C, which matches the ambient temperature range of 27–43 °C. The modulation range between the simulation and measurement differed because the suction temperature of 32.2 °C and the sub-cooler temperature of 32.2 °C in the calorimeter were set to measure the cooling capacity and to compare the capacity modulation under variations in the condensing temperature. That is, the condensing temperature was limited to over 32.2 °C in order to prevent the two-phase refrigerant from entering an expansion valve. The simulation results demonstrate that the capacity was modulated from 55% to 90%, and the inherent modulation was confirmed from 70% to 90% through the experiments. In that study, the ICM linear compressors secured the modulation response in terms of ambient temperature variations reflecting the required cooling demand of household refrigerators. However, the compressors did not require a stroke controller to realize the capacity modulation of a linear compressor. The absence of a controller can influence the energy efficiency of a linear compressor, depending on the ICM design, which is electrically non-resonated. The electric power consumption may be reduced by eliminating the electric controller or increased if the ICM design performs poorly. Hence, the present authors (Kim and Jeong, 2013) compared the performance of an ICM linear compressor with that of a conventional linear compressor in which an electrical resonance design was applied. The performance of the linear compressor was evaluated at an evaporating temperature of −26 °C and a condensing temperature of 38 °C. The conditions assumed were −18 °C for the freezer compartment and 30 °C for the ambient temperature; these were selected as the general operating conditions in household refrigerators. Although the required voltage, which is the driving force to generate the oscillating motion, was increased for the ICM linear compressor, the energy dissipation due to the current was nearly identical. Hence, the total efficiency of the ICM linear compressor was as high as that of an electrical resonant system.

On the other hand, linear compressors used in home refrigerators are subjected to a wide range of compression loads because of not only the variations of the ambient temperature, which affect the condensing temperature, but also those of the freezer compartment temperature, which affect the evaporating temperature. Research about the former case was introduced in the aforementioned study. The primary objective of the present study is to define the modulation characteristics of an inherent capacity-modulated linear compressor to evaporating temperature variations that again reproduces variations of the compartment temperature in a household refrigerator.

2. Theoretical analysis

2.1. Governing equations

A prototype compressor was made to realize both the conventional linear compressor and the inherent capacity modulated (ICM) linear compressor. A simple schematic diagram of the proposed linear compressor for a household refrigerator is illustrated in Fig. 1. The moving magnet of the linear motor generates an oscillating motion in the piston in a linear fashion. The piston in both systems is driven by the linear motor which moves from the top position (X_{top}, piston's top position) to the bottom position (X_{bot}, piston's bottom position). TDC (Top dead center) is the piston position when $X_{top} = 0$. When $X_{top} = 0$, the piston stroke is the maximum and the compressor gives the maximum cooling capacity. When X_{top} is greater than 0, the piston stroke is less than the maximum stroke and the cooling capacity decreases.

Details of the physical modeling and mathematical formulation for ICM linear compressors have been described in the present authors' previous papers (Kim et al., 2011; Kim and Jeong, 2013). These will be briefly described here. Eqs. (1)–(3) represent a mechanical, thermodynamic, and electric coupling system that can simulate the performance and the relevant dynamic characteristics of a linear compressor incorporated in a refrigeration system. The motion equation shown in Fig. 1 for the mechanical section coupled with both the thermodynamic section (F_{gas}) and the electrical section (α) can be described as follows:

$$m\frac{d^2x(t)}{dt^2} = -C_f\frac{dx(t)}{dt} - k_s[x(t) - X_o] + \alpha i(t) + F_{gas}(t), \quad (1)$$

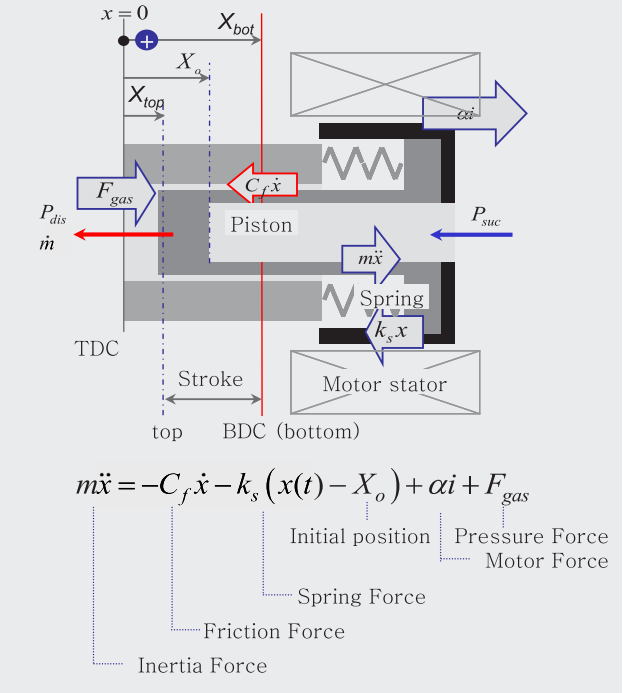

Fig. 1 – Schematic diagram of the proposed linear compressor.

where m is the piston mass, C_f is the viscous damping coefficient representing the effects of the oil friction between the piston and the cylinder wall, and k_s is the spring constant, representing the total stiffness of the tuning springs. In addition, α is the coefficient linking the thrust of the linear motor to the current ($i(t)$) in the coil.

The gas force acting on the piston results from the pressure difference between the compressed gas of inside the cylinder and suction gas of outside the cylinder, and it depends on the thermodynamic cycle. This can be expressed as the balance of the equivalent gas damping and the gas spring force, and is given by the following equation:

$$F_{gas}(t) = [P_c(t) - P_{suc}]A_p, \tag{2}$$

where A_p is the cross-sectional area of the piston, P_{suc} is the suction pressure under the assumption of an ideal compression cycle, and $P_c(t)$ is the time-varying pressure in the compression chamber.

Generally, the governing equation of the electric part in the linear compressor can be described by the following equation:

$$V(t) = L\frac{di(t)}{dt} + Ri(t) + \frac{1}{C}\int [i(t)]dt + \alpha\frac{dx(t)}{dt} \tag{3}$$

In this equation, the voltage source ($V(t)$), the resistance (R), the inductance (L), and the voltage induced by the motion of the magnet ($\alpha \cdot dx(t)/dt$: back electro-motive force: BEMF) are connected in series.

2.2. *Capacity change of the ICM linear compressor due to evaporating temperature variations*

The cooling demand of a refrigerator depends on the ambient temperature and the compartment temperature. For easier understanding, the cooling load of a freezer compartment is described as follows:

$$\dot{Q}_{CD,f} = \frac{T_{Amb} - T_F}{\sum R_{TH,f}}, \tag{4}$$

where $\dot{Q}_{CD,f}$ is the cooling demand of the freezer compartment, $\sum R_{TH,f}$ is the summation of the thermal resistance comprised of inner, middle, and outer wall of the freezer cabinet, T_F is the temperature inside the freezer compartment, and T_{Amb} is the ambient temperature.

The present authors (Kim et al., 2011; Kim and Jeong, 2013) proved that an inherent capacity-modulated linear compressor appropriately changes its capacity in accordance with the variations of the condensing temperature to suit the cooling demand change of the refrigerator without stroke controllers. They described the inherent capacity modulation under condensing temperature change representing ambient temperature variations. Also, Eq. (4) shows that the cooling demand increases as the compartment (refrigerator and freezer) temperature rises. The evaporating temperature varies because the evaporator surface is exposed to the compartment temperature. Eqs. (5) and (6) show the energy relationship between the inside and outside of the evaporator surface

$$\dot{Q}_{inside} = \dot{m}\Delta h \tag{5}$$

$$\dot{Q}_{eva} = UA(T_{eva} - T_{compartment}) \tag{6}$$

where $\dot{Q}_{inside}$ is the heat transfer rate of inside evaporator defined by $\dot{m}$ (mass flow rate) and the enthalpy difference between the inlet and outlet of an evaporator; $\dot{Q}_{eva}$ is the heat transfer rate through the evaporator; U is the total heat transfer coefficient comprised of the inside convection, medium conduction, and outside convection; T_{eva} is the evaporating temperature; and $T_{compartment}$ is the compartment temperature. The equation shows that both temperatures (evaporating and compartment temperature) either increase or decrease in the same way, in order to satisfy the energy balance, because the inside heat transfer rate delivered by the compressor needs to be maintained.

When the piston stroke and the piston's top position from the TDC are determined, the volumetric efficiency and the mass flow rate can be calculated from the following equations:

$$\eta_{vol} = \frac{\dot{m}_{mod}}{\dot{m}_{max}} = \frac{\rho(V_{1,mod} - V_{4,mod})f}{\rho V_{1,max} f} \approx \frac{\rho(V_{1,mod} - V_{4,mod})f}{\rho V_{1,mod} f} = 1 - \frac{V_{3,mod}}{V_{1,mod}}\left(\frac{P_{dis}}{P_{suc}}\right)^{1/k} = 1 - \frac{X_{top}}{X_{bot}}\left(\frac{P_{dis}}{P_{suc}}\right)^{1/k} \tag{7}$$

$$\dot{m}_{real} = \eta_{vol} \times \dot{m}_{max} = \left[1 - \frac{X_{top}}{X_{bot}}\left(\frac{P_{dis}}{P_{suc}}\right)^{1/k}\right] \times \rho A_p X_{bot} f \tag{8}$$

$$\dot{Q}_{mod} = \dot{m}_{mod}\Delta h, \tag{9}$$

where $\dot{m}_{mod}$ is the modulated mass flow rate, ρ is the density of the superheated refrigerant gas at the suction temperature and pressure, $V_{1,max}$ and $V_{1,mod}$ are the volume between X_{tdc} and X_{bot} in the maximum cooling capacity and in the modulated cooling capacity, respectively, $V_{3,mod}$ is the volume between X_{tdc} and X_{top} in the modulated cooling capacity, $V_{4,mod}$ is the re-expansion volume of $V_{3,mod}$, Δh is determined from the thermodynamic properties of the refrigerant, f is the input frequency applied to the linear motor, and $\dot{Q}_{mod}$ is the modulated cooling capacity. In equation (7), initial dead volume in the maximum cooling capacity is ignored because it is far smaller than the modulation volume ($V_{3,mod}$); $V_{1,max}$ is assumed to be $V_{1,mod}$ because the difference of two volumes ($V_{1,max} - V_{1,mod}$) is far smaller than the modulation volume ($V_{1,mod} - V_{4,mod}$). As shown in Fig. 1, the piston, driven by the linear motor, moves from the top (X_{top}) to the bottom position (X_{bot}). X_{tdc} ($X_{top} = 0$) is the allowable top position of a piston representing the full capacity of a linear compressor. The TDC position was inferred from the calculation with program and experiment. Experiments were carried out with a special controller to define TDC. After several tests, the TDC was determined as the minimum top clearance when the compressor gives the maximum cooling capacity. X_{top} has a positive value with driving capacity modulation due to the free piston mechanism of the linear compressor. Hence, the modulated capacity due to the evaporating temperature variations can be decisive if the stroke is defined.

$$\text{Stroke} = X_{bot} - X_{top} = (X_0 + L_D - X_{top}) \times 2 \tag{10}$$

where X_o is the initial position of the piston in the compression chamber, and L_D is the piston's drift length. A piston

moves back and forth in a linear fashion and the center position of the oscillation at no load condition is the same as the initial position. On the other hand, the center position of the piston oscillation is pushed back from the initial position as the pressure load by the compressed gas in a cylinder chamber increases. The push back length from the initial piston position is referred to the drift length. In order to define the drift length, Eq. (1) can be re-arranged as

$$m\ddot{x} + C_f\dot{x} - k_s(x - X_o) = \alpha i(t) + (\overline{P}_c - P_{suc})\cdot A_p \tag{11}$$

where $\alpha i(t)$ is the motor force, which is the external harmonic input, and $(\overline{P}_c - P_{suc})\cdot A_p$ is the averaged pressure force acting on the piston by the refrigerant gas in the compressor chamber. Based on the assumption that $x(t) = \overline{x} + x'(t)$, Eq. (11) can be divided into AC and DC terms, as follows:

$$m\ddot{x} + C_f\dot{x} - k_s x = \alpha i(t) \tag{12}$$

$$k_s(\overline{x} - X_o) = (\overline{P}_c - P_{suc})\cdot A_p \tag{13}$$

Hence, the drift length of the piston can be defined according to the following equation:

$$L_D = (\overline{x} - X_o) = \frac{(\overline{P}_c - P_{suc})\cdot A_p}{k_s}. \tag{14}$$

The length is proportional to the averaged gas force and anti-proportional to the mechanical spring stiffness; thus, the length increases when either the evaporating or condensing temperature is augmented. It is expected that the cooling capacity of the proposed compressor will be inherently modulated according to the evaporating temperature variations, in the same manner as found in the results for the condensing temperature variations. Theoretically, the modulation characteristics are not clear yet since the piston's top position is not defined. Both experimental and numerical solutions will used to verify the final modulation characteristics of the proposed linear compressor for the evaporating temperature variations; then, we will compare the results with those for the condensing temperature variations.

3. Experimental apparatus and conditions

3.1. *Experimental apparatus*

Fig. 2 provides a schematic diagram of the experimental apparatus used for the measurement of cooling capacity of the linear compressor. The system was designed to have a secondary refrigerant calorimeter which was presented in the standards of ISO 917. This equipment consists of a controller, a power meter for compressor, a power meter for calorimeter, a control switch, a suction pressure gauge in a range from 0 to 500 kPa at the inlet of the evaporator, a discharge pressure gauge in a range from 0 to 21,000 kPa at the outlet of the condenser, a thermocouple, and an expansion valve. This apparatus uses R600a as a refrigerant and covers the cooling capacity in a range from 100 to 600 W. Various data were measured in the experiments including temperatures and pressures at the suction and discharge ports, piston stroke, cooling capacity, voltage, current and input power. The maximum measurement error for temperature was 0.5 °C. A linear variable differential transformer is used to detect piston position and stroke. For the precise measurement of the piston position, the position sensor was calibrated and the maximum measurement error was 25.4 μm. The pressure measurement errors at low and high pressure were 1.87 and 3.74 kPa respectively. At a frequency of 60 Hz, the voltage, current, and power have absolute uncertainty from 0.03 to 0.22 V in the voltage range from 100 to 600 V, from 0.9 mA to 8.3 mA in the current range from 1.0 to 2.0 A, and from 0.1 to 0.2 W in the power range from 600 to 1200 W, respectively. In this system, the evaporator absorbs heat from the secondary refrigerant which gains energy from the electric heater in the "Calorie-tank". In the steady state, the cooling capacity of the evaporator remains at the same level with the input power to the electric heater. So, the input power to the electric heater in the calorie-tank was measured to obtain the cooling capacity and the measurement error was within 1.0%.

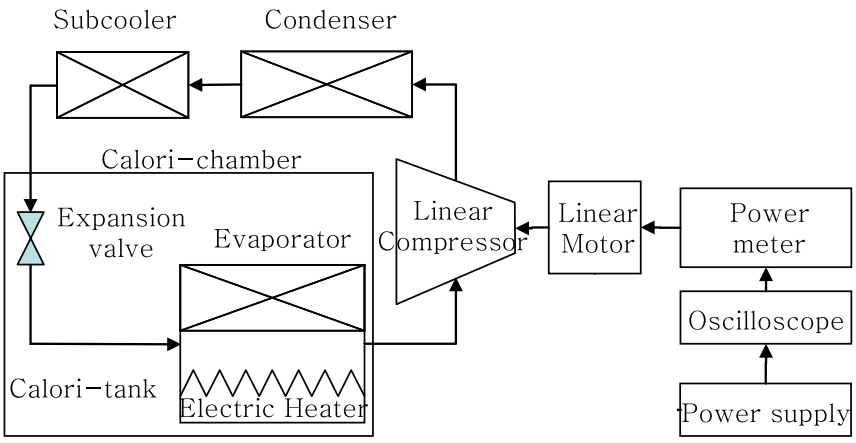

Fig. 2 – Experimental apparatus used to measure the COP of the refrigeration system.

3.2. Experimental conditions

The prototype compressor was evaluated over an evaporating temperature range of −35 to −15 °C, which corresponds to a freezer compartment temperature range of −27 to −7 °C. The results will be compared with those over a condensing temperature range of 30–50 °C, which corresponds to an ambient temperature range of 22–42 °C. Both temperatures have the same difference of 20 °C, in order to allow them to be compared based on the similar heat load introduced in Eq. (4). A suction temperature of 32.2 °C and sub-cooler temperature of 32.2 °C were set in order to measure the cooling capacity. The expansion valve is controlled by the information of suction pressure and suction temperature. A PID controller is used to catch up the target pressure and temperature from the current status. In this study, suction temperature was set as 32.2 °C and evaporating temperature was also set as fixed value for each test, and then the cooling capacity was measured. The capacity modulation characteristics for the variations of the condensing and evaporating temperatures were then investigated.

Table 1 shows the test conditions used to verify the modulation performance of the ICM linear compressor for the evaporating temperature variation. The condensing temperature was fixed at 38 °C, which corresponds to an ambient temperature of 30 °C. The test conditions shown in Table 2 were designed to verify the modulation performance of the ICM linear compressor for condensing temperature variation. The evaporating temperature was fixed at −26 °C, which corresponds to a freezer compartment temperature of −18 °C. The applied operating frequency and the voltage of the motor were 60 Hz and 180 V.

4. Results and discussion

4.1. Comparison between the simulated and measured values

Table 3 presents a comparison of the simulated and experimental results for the response characteristics (stroke representing cooling capacity, power factor and current representing power consumption) at all data points. At a supply power condition of 180 V and 60 Hz, the stroke amplitudes of the ICM linear compressor, obtained from the simulation and the experiment, were 18.02 mm and 17.88 mm, respectively; the difference was 0.8%. The power factor amplitudes, obtained from the simulation and the experiment, were 90.41% and 92.06%, respectively; the difference was −1.8%. The current levels representing the power consumed by the ICM linear compressor, obtained from the simulation and the experiment, were 0.560 A and 0.567 A, respectively; the difference was 1.3%.

As shown in Table 3, the model predicted the stroke of a piston within 2.2%. The power factor and current were predicted by the model to within 4.2% and 4.3% respectively.

Table 1 – Test conditions for the R600a refrigeration cycle to verify the evaporating temperature effect.

Property	Various specification conditions					
	Unit	No. 1	No. 2	No. 3	No. 4	No. 5
Suction temperature	[T1, °C]	32.2	32.2	32.2	32.2	32.2
Sub-cooler temperature	[T3, °C]	32.2	32.2	32.2	32.2	32.2
Condensing pressure	[kPa,]	503.6	503.6	503.6	503.6	503.6
Evaporating pressure	[kPa]	88.7	72.2	55.4	46.4	36.6
Condensing temperature	[T2, °C]	38.0	38.0	38.0	38.0	38.0
Evaporating temperature	[T4, °C]	−15.0	−20.0	−26.0	−30.0	−35.0
Supply frequency	[Hz]	60	60	60	60	60
Supply voltage	[V]	180	180	180	180	180

Table 2 – Test conditions for the R600a refrigeration cycle to verify the condensing temperature effect.

Property	Various specification conditions					
	Unit	No. 1	No. 2	No. 3	No. 4	No. 5
Suction temperature	[T1, °C]	32.2	32.2	32.2	32.2	32.2
Sub-cooler temperature	[T3, °C]	32.2	32.2	32.2	32.2	32.2
Condensing pressure	[kPa,]	404.5	464.6	503.6	604.2	684.6
Evaporating pressure	[kPa]	55.4	55.4	55.4	55.4	55.4
Condensing temperature	[T2, °C]	30.0	35.0	38.0	45.0	50.0
Evaporating temperature	[T4, °C]	−26.0	−26.0	−26.0	−26.0	−26.0
Supply frequency	[Hz]	60	60	60	60	60
Supply voltage	[V]	180	180	180	180	180

4.2. Response characteristics of the ICM linear compressor for evaporating and condensing temperature variations

The response characteristics of the ICM linear compressor under variations of the evaporating and condensing temperatures are compared in Figs. 3–10. All parameters (drift length, stroke, under-stroke, power factor, cooling capacity ratio, cooling capacity, density, and system resonant frequency) based on the predicted values have been plotted against temperature (x-axis) and the theoretical model was validated with the measured values in the previous section.

Fig. 3 shows the results for the drift length of a piston due to the variation of the evaporating and condensing temperatures. The length increased as both temperatures increased because the average pressure described in Eq. (13) increased. Fig. 3 shows the results for the drift length of a piston due to the variation of the evaporating and condensing temperatures. The drift length increases as both the evaporating and condensing temperatures increase because the average pressure described in Eq. (13) increases. The drift length increases from 0.72 to 1.06 mm for the evaporating temperature increment from −35 °C to −15 °C and increases from 0.80 to 0.93 mm for the condensing temperature increment of 20 °C. The rising slope for the evaporating temperature is steeper than that for

Table 3 – Comparison of the simulation and experimental results.

Property	Operating conditions (Temperature)		Comparison		
	Evaporating [°C]	Condensing [°C]	Simulation	Experiment	Discrepancy[a] [%]
Stroke [mm]	−26	35	17.86	17.68	1.0%
	−26	38	18.02	17.87	0.8%
	−26	45	18.36	18.40	−0.3%
	−26	50	18.54	18.86	−1.7%
	−15	38	18.09	17.70	2.2%
	−20	38	18.09	17.83	1.4%
	−26	38	18.02	17.87	0.8%
	−30	38	17.95	17.84	0.7%
Power factor [%]	−26	35	87.6	89.3	−1.9%
	−26	38	90.4	92.1	−1.8%
	−26	45	93.5	93.0	0.6%
	−26	50	94.8	91.0	4.2%
	−15	38	91.1	94.8	−3.8%
	−20	38	91.1	93.9	−3.0%
	−26	38	90.4	92.1	−1.8%
	−30	38	88.6	90.4	−2.0%
Current [A]	−26	35	0.532	0.542	−1.8%
	−26	38	0.560	0.567	−1.3%
	−26	45	0.652	0.652	0.0%
	−26	50	0.720	0.711	1.2%
	−15	38	0.712	0.682	4.3%
	−20	38	0.647	0.637	1.6%
	−26	38	0.560	0.567	−1.3%
	−30	38	0.500	0.512	−2.3%

[a] 100 × (Simulation − Experiment)/Experiment.

the condensing temperature because the density increment for the evaporating temperature is higher at the same conditions of the frontal area of a piston and spring stiffness.

In Fig. 4, the piston stroke increases as the condensing temperature increases similarly to the drift length shown in Fig. 3. However, the increasing slope deceases as the evaporating temperature increases and finally the stroke stop increasing. This can be interpreted by looking at the results of the under-stroke and power factor responses, shown in Figs. 5 and 6. When the evaporating temperature and the power factor (Fig. 6) increase, the under-stroke (Fig. 5) increases as well as the stroke (Fig. 4). Both responses increased the cooling capacity. When the power factor was constant, the stroke was constant and the under-stroke increased. The power factor generates power to run the piston and to overcome the resistive gas force acting on the piston's frontal surface. When the power factor was constant, the piston was pushed back by the gas force growth generated from both the condensing and the evaporating temperature. Hence, the stroke increment was stopped under the operating condition of increasing evaporating temperature.

The aforementioned analysis reflects the cooling capacity ratio shown in Fig. 7. The cooling capacity ratio (CCR) is defined as follows:

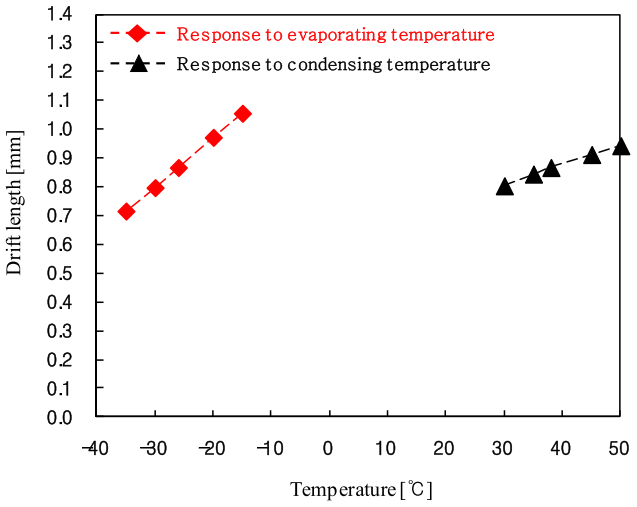

Fig. 3 – Drift length variation of a piston due to the evaporating and condensing temperatures.

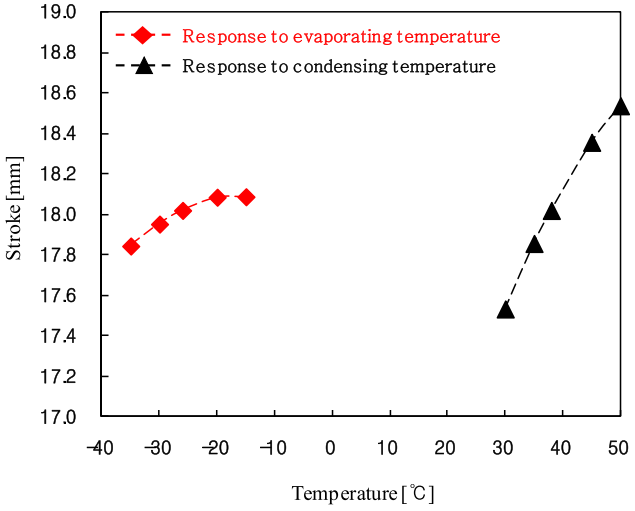

Fig. 4 – Stroke variation due to the evaporating and condensing temperatures.

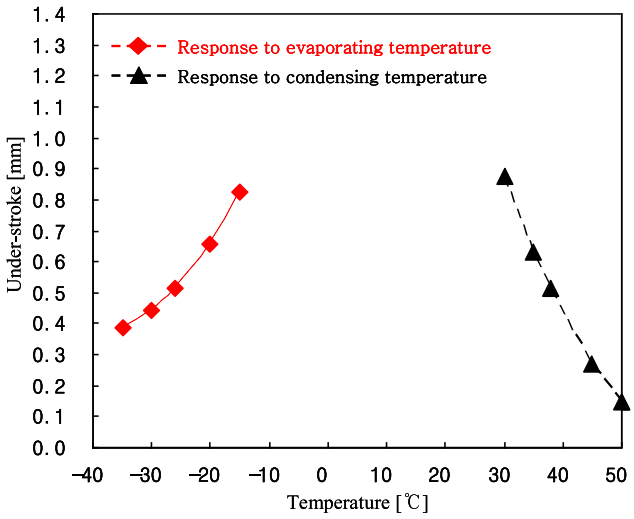

Fig. 5 – Under-stroke variation due to the evaporating and condensing temperatures.

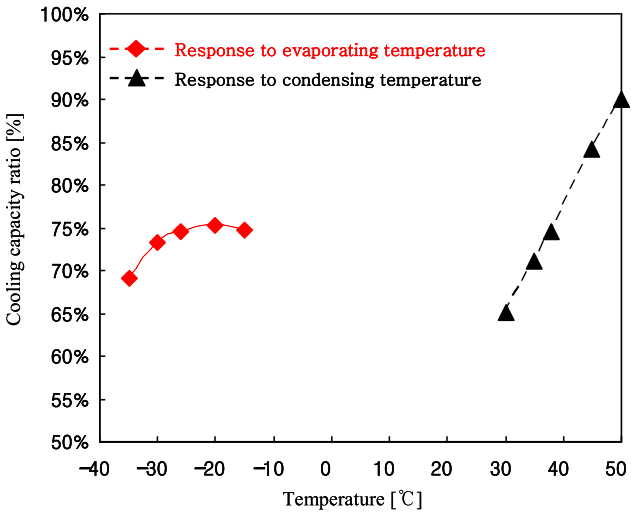

Fig. 7 – Cooling capacity ratio variation due to the evaporating and condensing temperatures.

$$CCR = \frac{Q_{mod}}{Q_{max}}, \tag{15}$$

where, $\dot{Q}_{max}$ is the maximum (full) cooling capacity. The cooling capacity ratio is equivalent to the capacity modulation ratio. When the condensing temperature increases in the range of 30–50 °C, the cooling capacity increases from 65 to 90%. On the other hand, the increase stopped at 75% for an evaporating temperature range of −15 to −35 °C.

Fig. 8 presents the cooling capacity responses due to the variations of the evaporating and condensing temperatures. The cooling capacity increased from 119 to 360 W for the evaporating temperature increment and increased from 191 to 241 W for a condensing temperature increment of 20 °C. Under a low load, such as for a condensing temperature of 30 °C, the power factor of motor was 81%, the stroke was 17.5 mm, and the cooling capacity ratio was 65%. Under high load conditions, such as for a condensing temperature of 50 °C, the power factor of motor was 95%, the stroke was 18.5 mm, and the cooling capacity ratio was 90%. It was verified that the capacity of a linear compressor can be self-modulated despite the absence of any stroke control unit.

In contrast, the increasing trend of both the stroke and the cooling capacity ratio for the evaporating temperature at the beginning stage (−35 °C) stopped from the middle stage (−25 °C) and then turned to the opposite trend in the ending stage (−15 °C). This means that the proposed compressor cannot be self-modulated according to the cooling demand assigned from the evaporating temperature variations. Interestingly, the cooling capacity increased from 119 to 360 W for the evaporating temperature increment of 20 °C, and this increment was larger than the increase from 191 to 241 W over a condensing temperature increment of 20 °C. These results can be interpreted by considering the density effect shown in Fig. 9. The density increased by 150.0% for an evaporating temperature increment of 20 °C and reduced by 6.5% for a

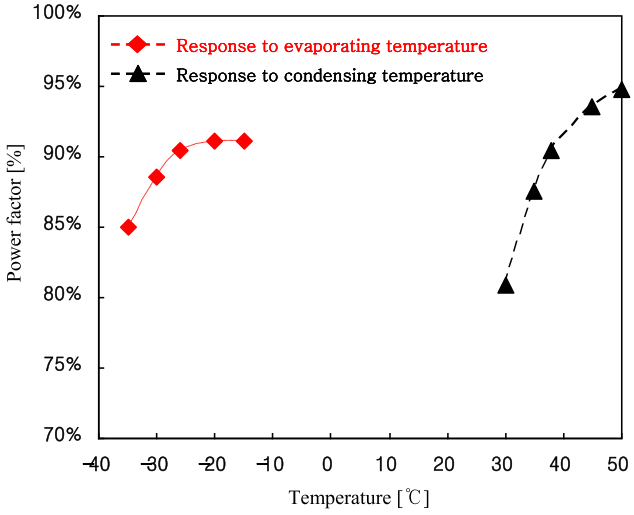

Fig. 6 – Power factor variation due to the evaporating and condensing temperatures.

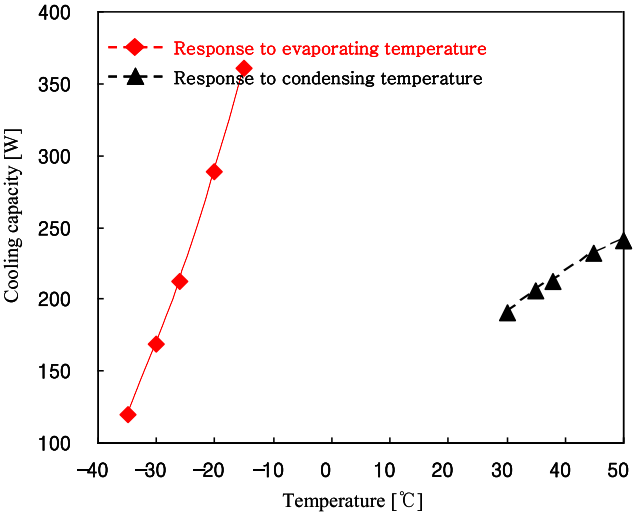

Fig. 8 – Cooling capacity variation due to the evaporating and condensing temperatures.

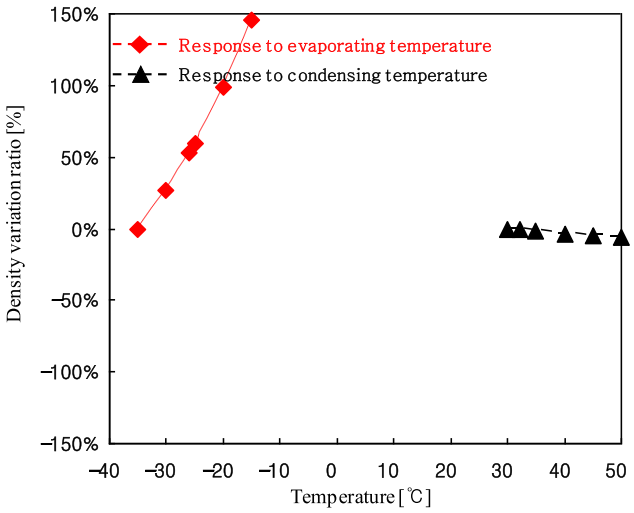

Fig. 9 – Density variation ratio due to the evaporating and condensing temperatures.

condensing temperature increment of 20 °C. The thermodynamic properties of R600a were obtained from the REFPROP database supplied by the National Institute of Standards and Technology.

Fig. 10 shows the system resonant frequency variations of the ICM linear compressor. The system for the variations of both temperatures reached the resonance state at a cooling capacity ratio of 73%. Also, the frequency increased from 59.5 to 60.5 Hz in a temperature range of 20 °C, as the average pressure in the compression chamber increased. The results of the two cases were nearly identical and imply the same running conditions in terms of mechanical resonant frequencies.

5. Conclusion

In this work, modulation characteristics of an inherent capacity-modulated linear compressor for condensing and evaporating temperature variations were investigated through numerical simulations and experiments. Among mechanical parts, a mass and spring were designed to realize a resonance system at general running conditions; that is, an evaporating temperature of −26 °C and a condensing temperature of 38 °C. A combination between inductance and capacitance for electrical parts was the key design of the self modulation technology. Under a low load, such as a condensing temperature of 30 °C, voltage lags current greatly, and hence the power factor is poor, meaning low capacity generation due to minimum electrical energy applied to the linear motor. In these conditions, the power factor was 81%, and the cooling capacity ratio was 65%. Under high load conditions, such as a condensing temperature of 50 °C, which is the maximum load condition, the voltage is almost in phase with the current, and so the power factor is almost 95%, meaning high capacity when high electrical energy is applied to the linear motor. Under these conditions, the cooling capacity ratio was 90%. It was verified that the capacity of a linear compressor can be self-modulated despite the absence of any stroke control unit.

In contrast, the increasing trend of both the stroke and the cooling capacity ratio for the evaporating temperature at the beginning stage (−35 °C) was diminished from the middle stage (−25 °C), and then stopped at the ending stage (−15 °C). This means that the proposed compressor cannot be self-modulated according to the cooling demand assigned from the evaporating temperature variations. Interestingly, the cooling capacity increased from 119 to 360 W for the evaporating temperature increment of 20 °C and the increase was larger than the increase from 191 to 241 W for a condensing temperature increment of 20 °C. These results were interpreted by considering the density effect. The density increased by 150.0% for an evaporating temperature increment of 20 °C and dropped by 6.5% for a condensing temperature increment of 20 °C. Hence, the main reasons for the capacity increment were the density change of the suction refrigerant for the evaporating temperature and the stroke of the piston for the condensing temperature.

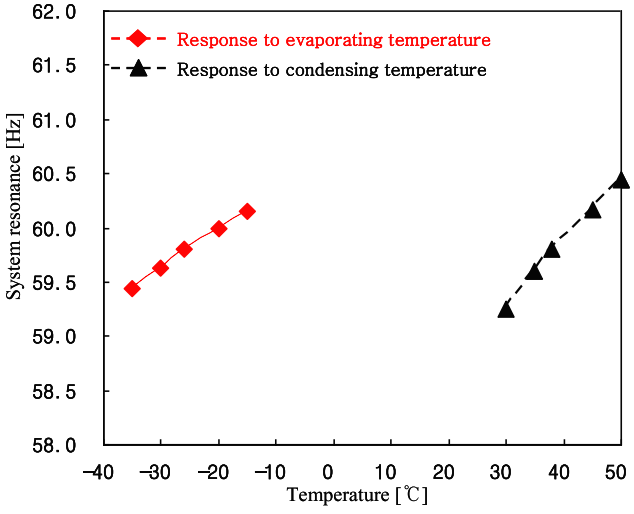

Fig. 10 – System resonance variation due to the evaporating and condensing temperatures.

REFERENCES

Bradshaw, C.R., Groll, E.A., Garimella, S.V., 2011. A comprehensive model of a miniature-scale linear compressor for electronics cooling. Int. J. Refrigeration 34 (1), 63–73.

Bradshaw, C.R., Groll, E.A., Garimella, S.V., 2013. Linear compressors for electronics cooling: energy recovery and its benefits. Int. J. Refrigeration 36 (7), 2007–2013.

ISO 917, 1989. Testing of Refrigerant Compressors. International Organization of Standardization, 1989(E).

Kim, J.K., Jeong, J.H., 2013. Performance characteristics of a capacity-modulated linear compressor for home refrigerators. Int. J. Refrigeration 36, 776–785.

Kim, H., Roh, C.K., Kim, J.K., 2009. An experimental and numerical study on dynamic characteristic of linear compressor in refrigeration system. Int. J. Refrigeration 32, 1536–1543.

Kim, J.K., Roh, C.K., Kim, H., Jeong, J.H., 2011. An experimental and numerical study on an inherent capacity modulated linear compressor for home refrigerators. Int. J. Refrigeration 34, 1415–1423.

Lee, H.K., Song, G.Y., Park, J.S., Hong, E.P., Jung, W.H., Park, K.B., 2000. Development of the linear compressor for a household refrigerator. In: Proceedings of International Compressor Engineering Conference. Purdue University, West Lafayette, USA.

Lee, H., Ki, S.H., Jung, S.S., Rhee, W.H., 2008. The innovative green technology for refrigerator. In: Proceedings International Compressor Engineering Conference. Purdue University, West Lafayette, Indiana, USA. Paper 1419(1–6).